Reviews of Modern Plasma Physics (2018) 2:5
https://doi.org/10.1007/s41614-018-0017-6

REVIEW PAPER

Recent progress in Asia-Pacific solar physics and astrophysics

Summary of the Solar/Astron session

P. F. Chen[1] · K. Shibata[2] · R. Matsumoto[3]

Received: 13 February 2018 / Accepted: 5 June 2018 / Published online: 18 June 2018

Abstract
More than 40 participants from the solar/astrophysical community attended the First Asia-Pacific Conference on Plasma Physics. Among them, four colleagues presented invited talks in the plenary session. In the Solar/Astron session, there were 23 invited talks and 14 contributed talks, with another two posters. These talks cover recent progress obtained in a wide spectrum of topics, including solar and galactic dynamo, solar and stellar flares, solar and galactic filaments, solar and astrophysical jets, solar and accretion disk winds, plasma waves and coronal heating, solar coronal mass ejections, magnetic reconnection in non-relativistic and relativistic regimes, star and planetary formation, shock–medium interactions, and even gravitational waves. Laboratory laser experiments and some new rocket and space missions were also introduced.

Keywords Solar physics · Astrophysics · Laboratory experiments

✉ P. F. Chen
chenpf@nju.edu.cn

K. Shibata
shibata@kwasan.kyoto-u.ac.jp

R. Matsumoto
matsumoto.ryoji@faculty.chiba-u.jp

[1] School of Astronomy and Space Science, Nanjing University, Nanjing 210023, China

[2] Kwasan and Hida Observatories, Kyoto University, Kyoto 607-8471, Japan

[3] Department of Physics, Chiba University, Chiba 263-8522, Japan

1 Introduction

We are living in such a unique corner of the universe, where most of the matter is in solid, liquid, or gas state. However, taking the universe as a whole, over 99.9% of the matter excluding dark matter is in the plasma state, including all the stars, galaxies, and the interstellar or intergalactic media. The dynamics and evolution of these plasmas are the research topics of astronomy, including solar physics, which focuses on various phenomena on the Sun. Different from laboratory plasma researchers who dream to have stable plasma confined by magnetic field (Li and Zhong 2018), astrophysicists, including solar physicists, are keen to study unstable magnetic configurations and the resulting eruptions.

There were about 40 participants in the Solar/Astron Session of the First Asia-Pacific Conference on Plasma Physics. The program of the conference can be found at http://aappsdpp.org/DPPProgramlatest. Four speakers from this session were recommended to give plenary talks. In the Solar/Astron session itself, there were 23 invited talks and 14 oral talks, with another 2 posters. These presentations cover a wide range, from the Sun to stars, and galaxies. This paper is aimed to summarize the main results of all the talks presented in the Solar/Astron Session.

2 Individual talks

Dynamo Magnetic field is an important aspect of plasma. Without magnetic field, the Sun would be a boring star, and there would be no any detectable change on the Sun in the lifetime of human beings. The Sun is actually so dynamic, with many types of eruptions, because of magnetic field. According to the dynamo theory, it is generally believed that the magnetic field of the Sun is generated by strong differential rotation in the solar interior, and then emerges to the solar surface with a period of ~11 years, which is called a solar cycle. During each cycle, the number of sunspots increases and then decreases. Similar cycles with different periods were detected in other solar-type stars (Wilson 1978; Choudhuri 2017).

Global-scale magnetohydrodynamic (MHD) simulations have been performed by many research groups to understand why and how the Sun and other stars produce cyclic magnetic activities. Before 2010, none of them succeeded in reproducing the clyclic behavior, e.g., the 11-year solar cycle. For the first time, Ghizaru et al. (2010) reproduced the cyclic polarity reversal in the solar convection zone. Masada and Sano (2016) extended the simulation to the solar atmosphere and found that large-scale structures of the vertical magnetic field are spontaneously formed at the solar surface only in cases with a strongly stratified atmosphere. They argued that the Rossby number is the crucial parameter which determines whether the large-scale MHD simulations can reproduce the cyclic dynamo (Masada and Sano 2018). The threshold is about 0.015–0.04 for the Rossby number inside the star, above which dynamo cannot be produced. Their work raised a question: how can we get the actual value of the Rossby number inside the stars from observations?

With a correct Rossby number, Hotta et al. (2016) performed MHD numerical simulations, where they found an intriguing phenomenon that is not expected from the mean-field theory for the dynamo: if the fluid and magnetic Reynolds numbers are small, an 11-year solar cycle can be reproduced, as shown in the top panel of Fig. 1. For medium Reynolds numbers, such a cycle disappears, as indicated by the middle panel of Fig. 1. For large Reynolds numbers, such a solar cycle appears again, as revealed by the bottom panel of Fig. 1. Motivated by these numerical results, Zhang and Fan (2018) investigated the dynamo theory and realized that in the mean-field dynamo theory, the α coefficient in the magnetic induction equation $\frac{\partial \langle B \rangle}{\partial t} = \nabla \times \Big(\langle u \rangle \times \langle B \rangle + \alpha \langle B \rangle - \beta \nabla \times \langle B \rangle \Big)$ is often taken to be $\alpha = -\frac{\tau}{3}(\overline{\mathbf{v} \cdot \nabla \times \mathbf{v}})$,

where τ is the velocity de-correlation time, and $\mathbf{v}$ is the velocity. As pointed out by

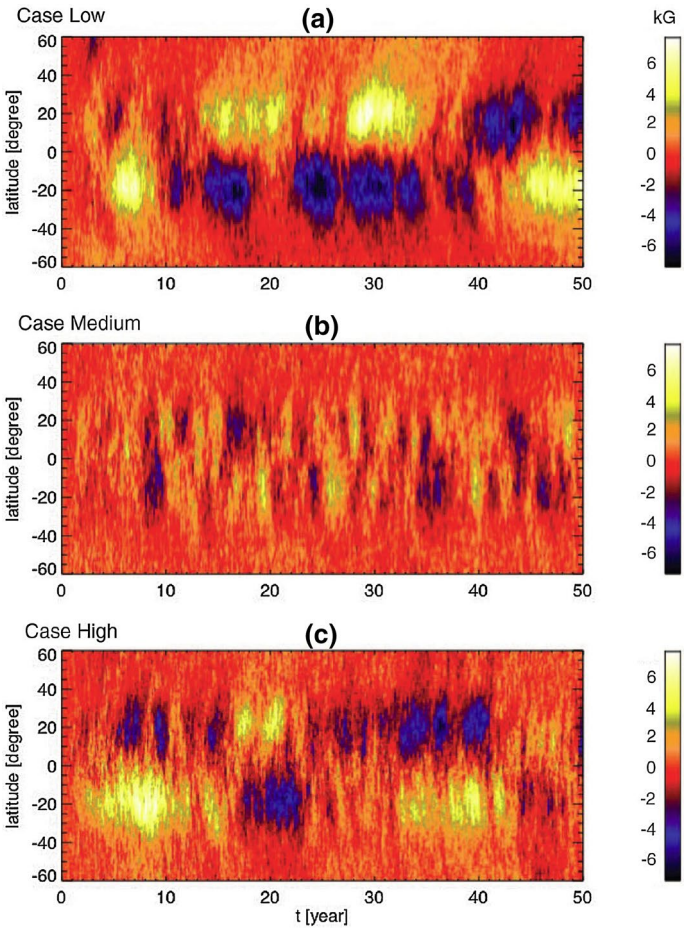

Fig. 1 Evolution of the toroidal magnetic field at the bottom of the convection zone in three cases with low (top panel), medium (middle panel), and high (bottom panel) Reynolds numbers. Taken from Hotta et al. (2016)

Pouquet et al. (1976), the α coefficient in the nonlinear dynamo theory should consist of two terms $\alpha = \frac{\tau}{3}(-\overline{\mathbf{v}\cdot\nabla\times\mathbf{v}} + \frac{\overline{\mathbf{B}\cdot\nabla\times\mathbf{B}}}{\mu_0\bar{\rho}})$, i.e., the kinetic helicity and magnetic field-related current helicity terms, and it is often assumed that the current helicity term is not important and hence neglected. On the basis of the MHD dynamo simulations performed by Fan and Fang (2014) and Zhang and Fan (2018) calculated the radial distributions of the kinetic and current helicity terms in the α coefficient and found that near the bottom of the convection zone, the magnetic term becomes dominant and should not be neglected. After considering the contribution of the current helicity term in the α coefficient, they can naturally explain why the solar cycle can be reproduced in the case of small Reynolds number (e.g., $Re = 323$), and the cyclic behavior disappears when the Reynolds number is medium (e.g., $Re = 382$), but the solar cycle resumes when the Reynolds number becomes larger, e.g., $Re = 2000$.

Helicity of solar filaments From the above description, we can see that current helicity $H_c = (\mathbf{B}\cdot\nabla\times\mathbf{B})/\mu_0$ is a very important quantity in describing the evolution of the magnetic field. In the solar wind turbulence, the existence of helicity leads to one-chiral-sector-dominated states (Zhu 2017). On the solar surface, interestingly it is found that current helicity shows a persistent pattern in each hemisphere, i.e., it is predominantly negative in the Northern Hemisphere and positive in the Southern Hemisphere. The straightforward way to determine the sign of current helicity is to make use of the vector magnetograms of solar active regions (Seehafer 1990). However, one problem of the magnetic measurement is the 180° ambiguity in the azimuthal angle. Alternatively, several indirect methods have been proposed to infer the sign of helicity based on imaging observations only, as summarized by Martin (1998). One of the patterns is the orientation of the filament barbs, i.e., left bearing or right bearing, and it was proposed that there is a one-to-one correspondence between the left-/right-bearing barbs and positive/negative helicity of the filaments (Martin et al. 1994). Such a correspondence is called Martin's rule later. Guo et al. (2010) and Chen et al. (2014b) challenged this correspondence and argued that the one-to-one correspondence claimed by Martin et al. (1994) holds only for the inverse-polarity filaments, i.e., those supported by magnetic flux ropes. However, for the normal-polarity filaments, i.e., those supported by magnetic sheared arcades, the one-to-one correspondence is exactly opposite. Therefore, it seems that we cannot determine the sign of helicity based on the bearing sense of filaments barbs. On the contrary, another pattern related to solar filaments was discovered (Chen et al. 2014b): once a filament erupts, part of the cool material drains down to the solar surface along the threading magnetic field lines, forming two conjugate brightenings, as indicated by the green circles in Fig. 2. Relative to the magnetic neutral line, the two brightenings are either left skewed or right skewed. Chen et al. (2014b) proposed that there is one-to-one correspondence between the left-/right-skewed drainage sites and negative/positive helicity of the filaments, as illustrated in Fig. 2.

Using the skew of the filament drainage sites as the tracer of the sign of helicity, Ouyang et al. (2017) surveyed all the erupting filaments observed by the Solar Dynamics Observatory (SDO) satellite during 2010–2015, and found that 91.6% of the erupting filaments follow the hemispheric rule of helicity sign, i.e.,

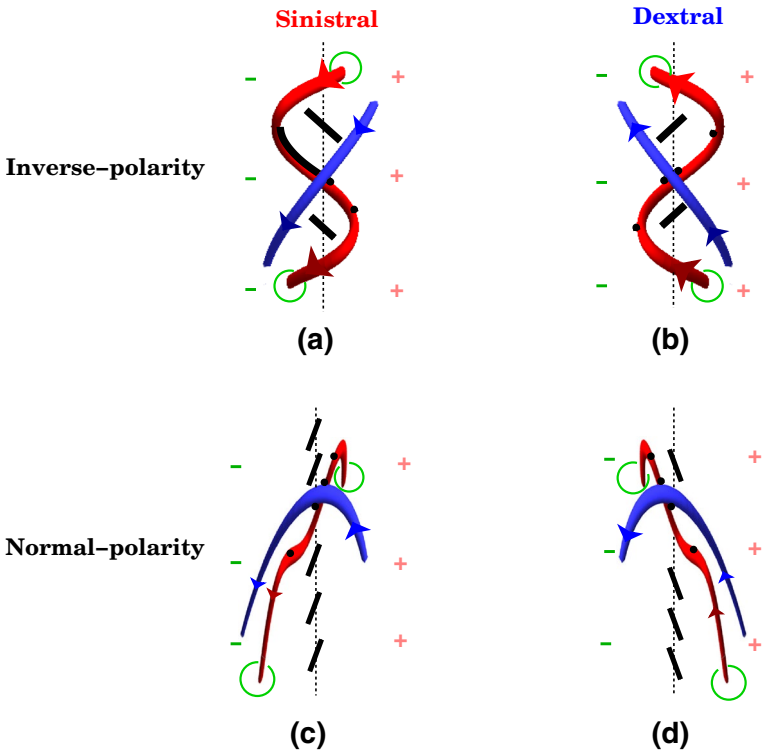

Fig. 2 Skew of the drainage sites and sign of helicity. Taken from Chen et al. (2014b)

negative in the Northern Hemisphere and positive in the Southern Hemisphere. They also investigated the yearly variation of the strength of the hemispheric rule of helicity sign. It was revealed that the strength of the hemispheric preference of the quiescent filaments decreases slightly from 97% in the ascending phase to 85% in the descending phase of solar cycle 24, whereas the strength of the intermediate filaments keeps a high value around $96 \pm 4\%$ at all times. The active-region filaments, however, show significant variations, with their strength of the hemispheric preference rising from 63 to 95% in the rising phase, and remaining at $82 \pm 5\%$ during the declining phase. The yearly variation of the strength of the hemispheric rule for all the filaments and the three categories of filaments are illustrated in Fig. 3, respectively.

Furthermore, Chen et al. (2014b) proposed an indirect method to determine whether a filament is supported by a flux rope or by a sheared arcade without measuring the coronal magnetic field, i.e., if the filament barbs and the sign of helicity follow Martin's rule, the magnetic field supporting the filament is a flux rope; if the filament barbs and the sign of helicity are opposite to Martin's rule, the magnetic field is a sheared arcade. Applying this method to the 571 erupting filaments observed by the SDO satellite during 2010–2015, Ouyang et al. (2017)

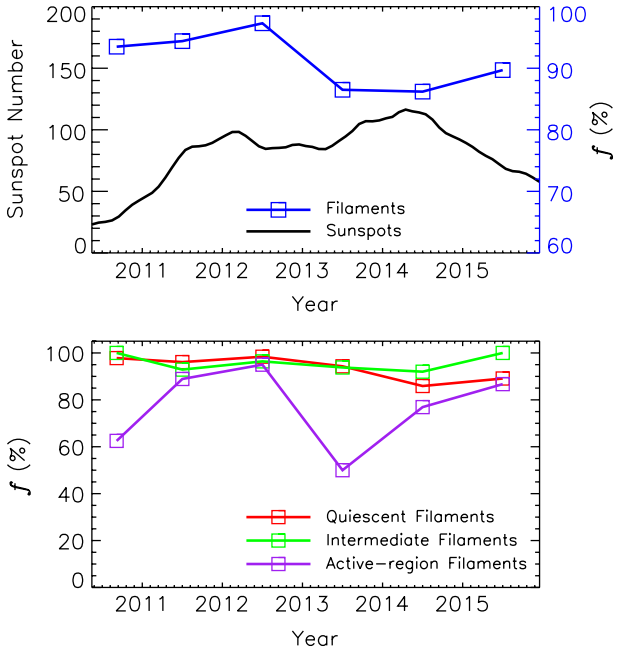

Fig. 3 Top panel: cyclic evolution of the sunspot number (black line) and, f, the strength of the hemispheric rule obeyed by the filament chirality (connected blue squares). Bottom panel: cyclic evolution of f for the quiescent filaments (connected red squares), intermediate filaments (connected green squares), and active-region filaments (connected purple squares). Taken from Ouyang et al. (2017)

found that 89% of the sample are supported by a magnetic flux rope (i.e., these are inverse-polarity filaments), and 11% of the sample are supported by a magnetic sheared arcade (i.e., these are normal-polarity filaments).

Rayleigh–Taylor instability in solar filaments As cold dense material (with $T \sim 10^4$ K and $n \sim 10^{11}$ cm^{-3}) suspended in the hot tenuous corona (with $T \sim 10^6$ K and $n \sim 10^9$ cm^{-3}), solar filaments may survive for days or weeks. On erupting, they produce solar flares and coronal mass ejections (CMEs). Even before eruption, because of the ever evolving solar surface and the intrinsic instabilities, a filament shows various dynamics (Hillier 2018), such as counterstreaming (Shen et al. 2015), propagating waves (Okamoto et al. 2015), and upward-moving plumes (Berger et al. 2008). It was proposed that the upward-moving plumes are due to the Rayleigh–Taylor instability (Ryutova et al. 2010). Hillier et al. (2012a) performed three-dimensional (3D) MHD simulations of quiescent filaments which are supported by dipped magnetic field lines. As illustrated in Fig. 4, the simulations obtained rising plumes with a velocity of ~8 km s^{-1} and a length of $\sim 10^3$ km, which are both comparable with the observations.

After the initial exponential growth of the instability, the dynamics of the plumes becomes nonlinear. The simulated nonlinear flow solution could be used to estimate the compression of the plume plasma and hence the plasma β of the filament (Hillier et al. 2012b).

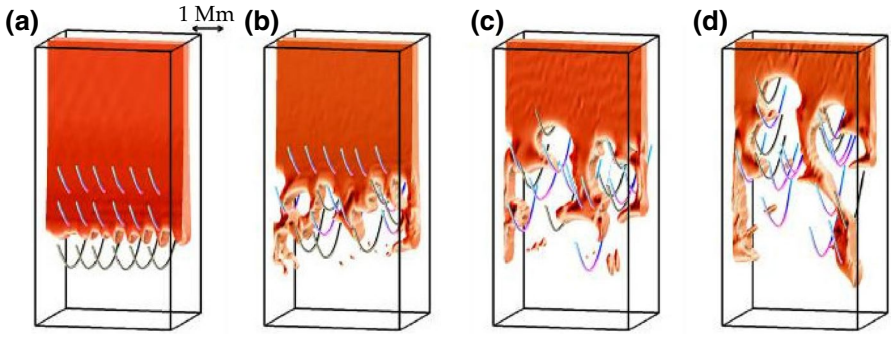

Fig. 4 Evolution of the plasma density and magnetic field in the 3D MHD simulation of the magnetic Rayleigh–Taylor instability of a solar filament, showing rising plumes with a length of $\sim 10^3$ km. Taken from Hillier et al. (2012a)

Filaments in galaxy clusters Except for some solar filaments which are formed via direct injection of cold plasma from the chromosphere to the hot corona (Zou et al. 2017), many solar filaments are formed via thermal instability of the hot material in the corona. Since the galaxy clusters have also a hot corona with a temperature of 10^7–10^8 K, thermal instability happens there as well. Although the cooling timescale is much smaller than the age of the clusters, the whole cluster corona did not collapse and only some cold filamentary structures were observed. It means that some heating mechanisms are working to balance the radiative cooling.

The feedback from active galactic nuclei (AGN) has been proposed to play an important role in regulating the intracluster media. Prasad et al. (2015, 2017) performed 2D and 3D hydrodynamic simulations, and the numerical results verified such a paradigm: local cooling happens to form cool cores. Because of gravity, these cores are accreted into the supermassive black hole at the center of the dominant cluster galaxy. The enhanced mass accretion powers the AGN jets, as illustrated in Fig. 5. These relativistic jets heat the intracluster medium, closing a feedback loop that efficiently prevents the otherwise runaway thermal instability in the cool cores. Prasad et al. (2015) further pointed out that, to allow such a feedback loop to work well, the ratio of the cooling time to the free-fall time should be less than 10.

Future efforts are needed to extend the hydrodynamic simulations to MHD simulations, where the inclusion of magnetic field leads to anisotropic heat conduction and several other instabilities.

Coronal heating One of the biggest puzzles yet to be solved in astrophysics is how the solar corona is heated to 1–2 MK, two orders of magnitude higher than that of the solar surface, which is ~5700 K. Since it has been well known that the dissipated energy comes from nonpotential magnetic field, i.e., the magnetic field with electric currents, the dissipation mechanisms are then classified into magnetic reconnection model and Alfvén wave model, depending on their direct current and alternative current nature (Klimchuk 2015). Whereas no reconnection model supporters attended this meeting, several participants delivered talks on the Alfvén wave model.

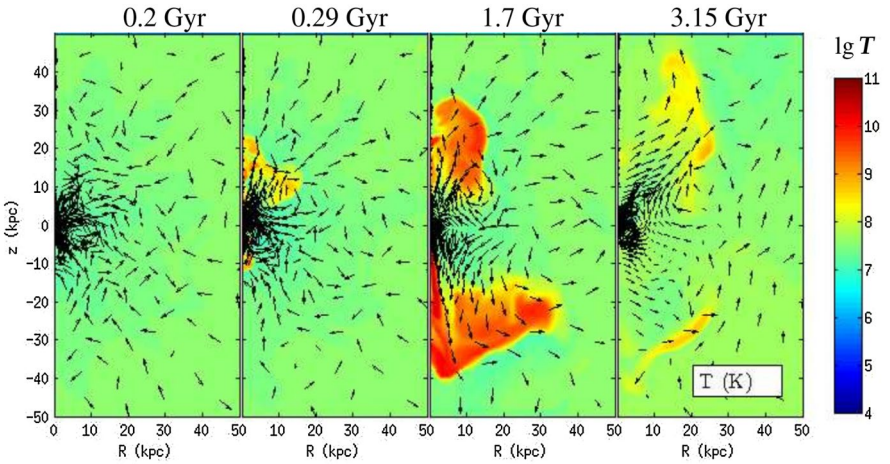

Fig. 5 Evolution of the temperature (color) and the velocity (arrows) in the hydrodynamic simulation of plasma accretion and AGN jets. Adapted from Prasad et al. (2015)

Okamoto et al. (2015) presented the analysis of an oscillating prominence observed in Ca II H and Si IV lines. They argued that the prominence oscillation was due to propagating Alfvén waves. As the amplitude of the waves decreases, the Ca II H emission, with a formation temperature of 0.1 MK, becomes fainter and fainter along the prominence threads. At the same time, the Si IV intensity (with a formation temperature of 0.8 MK) becomes stronger and stronger. Such a coincidence, as shown in Fig. 6, indicates that the energy in the observed waves is converted to the thermal energy of the prominence plasma. With 3D MHD simulations, Okamoto et al. (2015) found that the prominence oscillation excites Kelvin–Helmholtz instability near the boundary of the oscillating threads, forming numerous thin current sheets. The wave energy is dissipated in these current

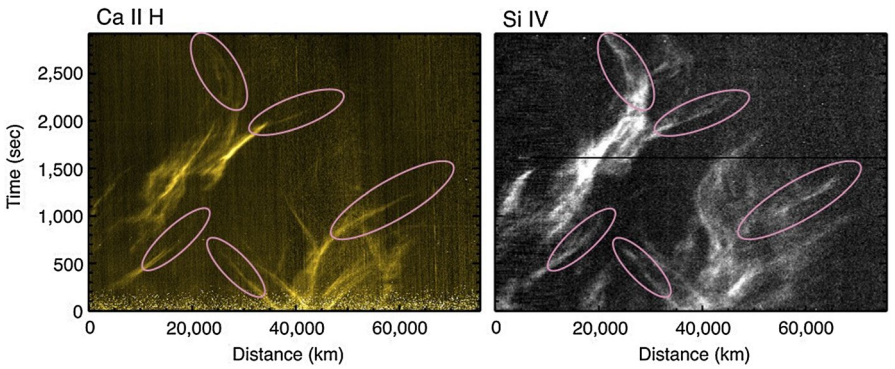

Fig. 6 Simultaneous Ca II H and Si IV images of a prominence, where the ellipses mark the heating of the prominence threads as waves are damping. Taken from Okamoto et al. (2015)

sheets. They claimed that the observations provide direct evidence for wave heating of the solar corona.

Waves are ubiquitous in the turbulent solar atmosphere. As in any other turbulence, large-scale MHD waves would cascade down to kinetic waves (Voitenko and de Keyser 2011), where the wave energy is ultimately dissipated. Chen and Wu described such a picture in their talk. They showed how MHD Alfvén waves can be nonlinearly converted to kinetic Alfvén waves (Zhao et al. 2014), how kinetic Alfvén waves are excited by density striation (Wu and Chen 2013), and how kinetic Alfvén waves can be excited by fast electron beams (Chen et al. 2014a). Their recent analysis indicates that ion beams might be more efficient in generating kinetic Alfvén waves than electron beams (Xiang et al. 2018).

The thermal and dynamic features of the coronal structures, such as coronal loops, provide observable constraints for any heating mechanism. By analyzing the spectroscopic data from the Hinode satellite and comparing the observed loops with the extrapolated magnetic loops, Xie et al. (2017) found that (1) most of the coronal loops are not in a hydrostatic equilibrium; (2) the coronal loops are nearly isothermal along the line of sight; (3) the temperature distribution along most loops is flat in the coronal part; (4) the nonthermal velocity in the cold and warm loops is in the range of 3–48 km s^{-1}, and (5) the filling factor of the coronal loops is between 8 and 89%. The authors concluded that Alfvén wave turbulence model is presumably responsible for heating these loops.

Chromospheric jets Collimated jets have been observed in different layers of the solar atmosphere. For the hot coronal and transition-region jets (Tian et al. 2014), magnetic reconnection has been proposed to be the driving mechanism (Shibata et al. 1992). For the chromospheric jets, whereas some of them might be due to magnetic reconnection as well (Shibata et al. 2007), others seem to be driven by waves, either slow-mode waves or Alfvén waves. Iijima and Yokoyama (2015) carried out 2D radiation MHD simulations where chromospheric jets can be produced by shocks passing through the transition region. They found that the coronal temperature is crucial in determining the height of the chromospheric jets: the jets become taller for lower coronal temperature (such as in coronal holes), and they are shorter for higher coronal temperature (such as in active regions). However, these jets have a typical height of 6–8 Mm only, which is not tall enough to reproduce the observed height up to 10 Mm.

In their recent 3D radiation MHD simulations, Iijima and Yokoyama (2017) succeeded in generating chromospheric jets as tall as 10 Mm, as displayed in Fig. 7. The reason is that torsional Alfvén waves are excited in 3D, which provide strong enough lifting force for tall spicules or chromospheric jets. It was also revealed that jets are formed in clusters with the diameter of several Mm, and each jet can be considered as a fine structure in the cluster.

Solar flares Various quasi-periodic pulsations (QPPs) have been discovered in association with solar flares. Generally, the period is in the range from a fraction of a second to several minutes. However, Tan and Tan (2012) found a type of QPPs in microwaves with a period of a few milliseconds. Most of these millisecond bursts are clusters of spike bursts, and others are similar to type III radio bursts. They proposed a model to explain these millisecond radio bursts: The tearing-mode

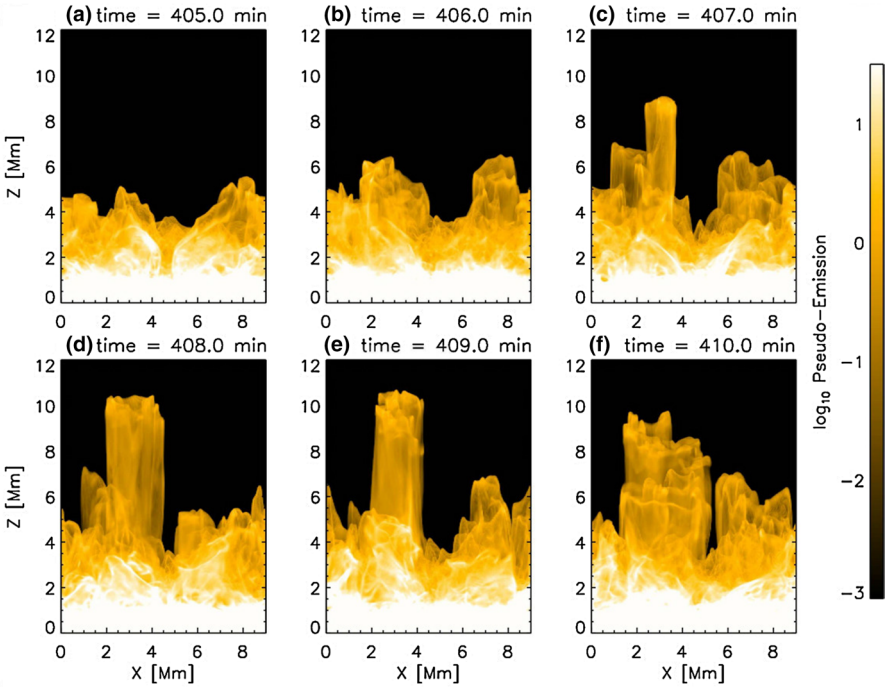

Fig. 7 Six snapshots of the synthesized chromospheric images showing the generation of tall jets. Taken from Iijima and Yokoyama (2017)

instability in the reconnection current sheet produces many small magnetic islands, which are conveyed to the flare loop along the reconnection outflow. Small-scale reconnection may happen at the X-point between neighboring magnetic islands, which accelerates electrons. The electrons accelerated by these merging magnetic islands are responsible for the millisecond microwave bursts, as illustrated in Fig. 8.

The classical picture of solar flares is as follows: Magnetic energy, which is built up gradually in the corona via emerging magnetic flux and solar surface motions, is suddenly released and is converted to the kinetic and thermal energies of the plasma, as well as nonthermal energy of the relativistic particles. According to this picture, the solar photosphere, where the plasma β is much larger than unity, is the driving source of the free energy of the coronal magnetic field. However, Bi et al. (2016, 2017) reported that, during an X1.6-class flare, the sunspot reverses its rotation from counterclockwise to clockwise rapidly. With the help of coronal magnetic field extrapolation, they argued that the reversal of the sunspot rotation is driven by a Lorentz torque after magnetic twist is transformed from the reconnection site to the solar surface. It seems that solar flares, as a consequence of the release of magnetic energy accumulating in the corona via photospheric motions and flux emergence, can provide back reaction to the solar photosphere.

Superflares Solar flares have a typical energy range of 10^{29}–10^{32} erg. The strong flares, together with the associated CMEs, can be hazardous to the space environment near the Earth, producing damages to the satellites, telecommunication,

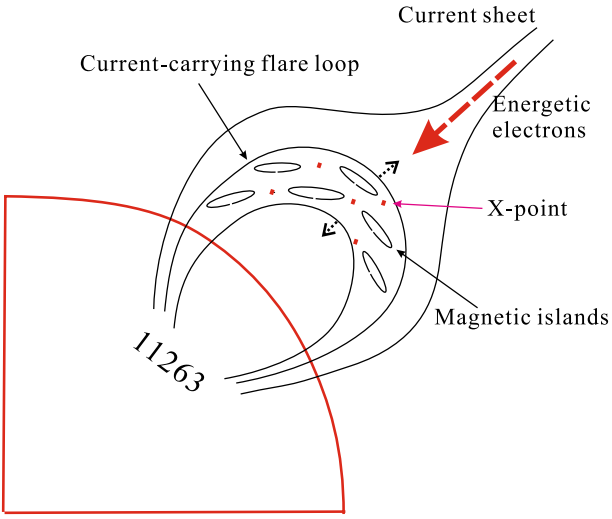

Fig. 8 Schematic sketch explaining that millisecond radio bursts are produced by downward moving electrons crossing magnetic islands inside the flare loop. Taken from Tan and Tan (2012)

navigation, power grids on the Earth, and so on. Therefore, one critical question is: will our Sun produce superflares which are much more energetic than the largest flare we have observed so far?

To answer this question, Shibata et al. (2013) used a sample of 365 superflares observed from ~83,000 solar-type stars by the Kepler mission over 120 days (Maehara et al. 2012) and calculated the superflare occurrence frequency as a function of flare energy. The occurrence frequency of superflares is then compared with the occurrence frequency distribution of solar flares and microflares. As shown in Fig. 9, the superflares on solar-type stars follow almost the same power-law distribution as

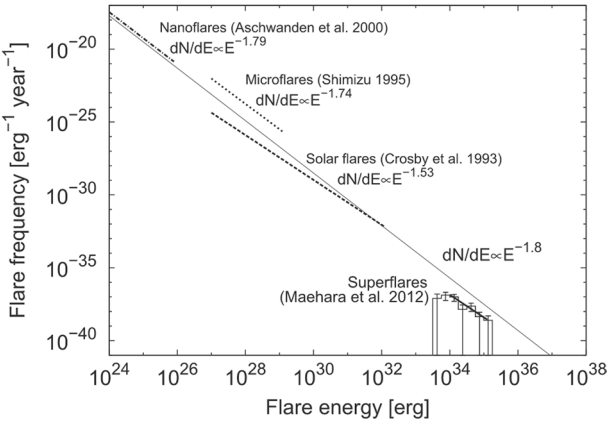

Fig. 9 Comparison between the occurrence frequency of superflares and that of solar flares at different energies. Taken from Shibata et al. (2013)

the solar flares and microflares. Such a power-law distribution implies that there is a possibility that superflares with energy of 10^{34} erg would occur once every 800 years on our Sun. According to the plenary talk given by Shibata, if such a superflare happens on the Sun, the consequence is catastrophic:

- All artificial satellites would be damaged.
- All astronauts and some of the airline passengers would be exposed to fatal radiation.
- Ozone layer depletion would occur.
- Radio communication trouble would occur all over the world.
- Global blackout would occur all over the Earth.
- All nuclear power stations would lose electricity and hence be in a state of meltdown.

Solar eruption forecast As mentioned above, solar eruptions may pose hazardous damages to human activities. Therefore, a critical question is: what determines when, where, and how big solar eruptions occur? Accurate prediction of solar eruptions is not only beneficial for protecting our society, but also reflects how correctly we have understood the physics of solar eruptions.

In his plenary talk, Kusano reviewed the efforts of his group in numerical forecasting of solar eruptions. The triggering of CMEs is often associated with the injection of new magnetic flux from the solar interior into the solar atmosphere (Feynman and Martin 1995; Chen and Shibata 2000). Kusano et al. (2012) conducted a simulation survey with different types of magnetic structures by changing the shear angle (θ_0) of the initial linear force-free magnetic field and the azimuthal orientation (ϕ_e) of the small-scale injected field. It is revealed that two types of magnetic structures favor the onset of solar eruptions, i.e., magnetic flux reversed to the envelope magnetic field and that reversed to the core magnetic field. This model was recently applied to the observational data-constrained simulations (Muhamad et al. 2017), which explains the observations very well (see Fig. 10).

Recently, they defined a new instability, called the double arc instability (Ishiguro and Kusano 2017). The critical parameter for this instability is $\kappa \equiv T_{\rm w} \frac{\phi_{\rm rec}}{\phi_{\rm tot}}$, where T_w is the magnetic twist of the reconnected double magnetic loops, $\phi_{\rm rec}$ is the reconnected magnetic flux, and $\phi_{\rm tot}$ is the total magnetic flux. They suggest that if κ is greater than the threshold $\kappa_0 \sim 0.1$, the double arcs would erupt even if the condition for the torus instability is not satisfied.

Solar wind Because of the low collision rate and the ubiquitous waves, the solar wind plasma is never in a thermal equilibrium state. As a result, the energy spectrum of the solar wind, in particular the fast solar wind, is far from a Maxwellian distribution: in addition to a Maxwellian core with an energy of $E \sim 5$ eV near the Earth orbit, there is an isotropic halo component at 0.1 keV $< E <$ 2 keV, an antisunward strahl component at 0.1 keV $< E <$ 2 keV, and a superhalo component at 2 keV $< E <$ 200 keV (Lin 1998). Tao et al. (2016) presented a statistical survey of the suprathermal strahl and halo electrons. It was found that both of them can be fit by the kappa distributions. These authors found a strong positive correlation

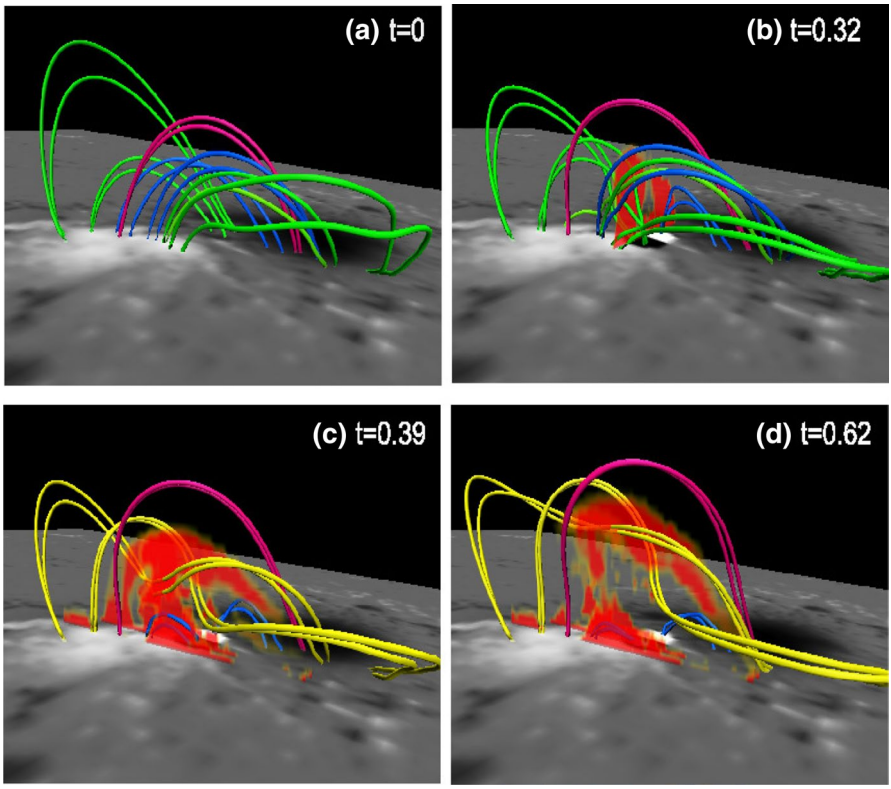

Fig. 10 Numerical simulation of a coronal mass ejection triggered by emerging magnetic flux whose polarity orientation is opposite to the background magnetic field, where the colored lines correspond to the magnetic field. Taken from Muhamad et al. (2017)

between the number densities of the strahl and halo electrons, but both of them have no clear association with the core population. They also conducted a similar survey on the superhalo electrons as well (Wang et al. 2015). These electrons present a power-law distribution in energy and an isotropic distribution in space. Both the power index and the number density are not correlated with the sunspot number, nor with the solar wind core population. These authors proposed that the superhalo electrons may originate from magnetic reconnection at the solar wind source site, although they cannot exclude the possibility that these electrons result from the wave–particle interactions while propagating in the interplanetary medium.

The velocity difference between the halo and core components, as well as the temperature anisotropy, is a free energy source of kinetic instabilities that drive electromagnetic fluctuations and waves in microscales. With particle-in-cell (PIC) simulations, Seough et al. (2015) demonstrated that unidirectionally propagating whistler waves are naturally generated in situ by the whistler instability, which results from either the relative core–halo drift velocity or mildly anisotropic electrons. Seough et al. (2015) also demonstrated a scenario for the formation of strahl electrons: the

enhanced whistler waves scatter some of the halo electrons moving in the anti-sunward direction. The remaining anti-sunward moving halo electrons, which are not scattered, form the field-aligned strahl electrons.

Relativistic magnetic reconnection As an efficient mechanism to convert magnetic energy to thermal and kinetic energies, magnetic reconnection has been extended from solar flares to many other astrophysical phenomena, such as astrophysical jets, pulsar wind, and gamma-ray bursts (GRBs), where the Poynting flux overwhelms the mechanical energy of the plasma. To explain the extremely high energy conversion rate in these phenomena, it has been proposed that turbulence plays an important role in magnetic reconnection so that the reconnection rate is nearly independent of the plasma resistivity, which is very small. This idea was verified in non-relativistic incompressible MHD simulations with plasma β larger than unity. Takamoto et al. (2015) extended the previous work to the relativistic regime with 3D MHD simulations. They found that only 1% of the magnetic energy is sufficient to drive turbulent reconnection, and similar to the non-relativistic case the reconnection rate is independent of the plasma resistivity owing to the turbulence. They also found that when the Alfvén Mach number reaches ~0.3, the compressibility of the plasma cannot be neglected since compressibility tends to reduce the reconnection rate. In a following paper (Takamoto and Lazarian 2016), they argued that in a Poynting flux-dominated turbulent plasma, fast and Alfvén modes are strongly coupled, so that the two modes should not be treated separately as had been done in the non-relativistic case.

Radiation may also play an important role in relativistic magnetic reconnection. After considering the optically thin synchrontron radiation in a 2D MHD simulation, Takeshige et al. (2018) demonstrated that the inclusion of radiation can efficiently enhance the reconnection rate. It is revealed that when the cooling timescale is smaller than 10–100 times the Alfvén timescale, the plasma β in the inflow region would decrease.

General relativistic MHD near compact objects Near compact massive objects such as black holes and neutron stars, general relativity should be considered. Takahashi et al. (2016) first performed 3D general relativistic radiation MHD (GRRMHD) simulations of the accretion flow near a black hole with a mass of ten times the solar mass, as illustrated in Fig. 11. They reported that the relatively cold disk ($T \sim 10^7$ K) is truncated at ~10–30 times the Shwarzschild radius, while the overheated ($T > 10^9$ K) tenuous gas fills in this area and extends away from the black hole to sandwich the cold disk. The numerical results are consistent with the observations of the accretion disks in the very high state. When the accretion rate exceeds the Eddington accretion rate, the radiation accelerates the outflow with a terminal velocity of $0.3c$ in the polar directions. Subject to the Rayleigh–Taylor instability, the outflow crushes into a clumpy structure, which may be the origin of the X-ray variability with a timescale of 50 s. For moderately high accretion cases, arc-shaped non-axisymmetric density enhancements are formed in the accretion disk, whose rotation may explain the high-frequency quasi-periodic oscillations (QPOs).

Later, Takahashi and Ohsuga (2017) performed 2.5D GRRMHD simulations of the accretion process near a non-rotating magnetized neutron star. It was found that, owing to the dipole magnetic field, the accretion disk is truncated at a distance of

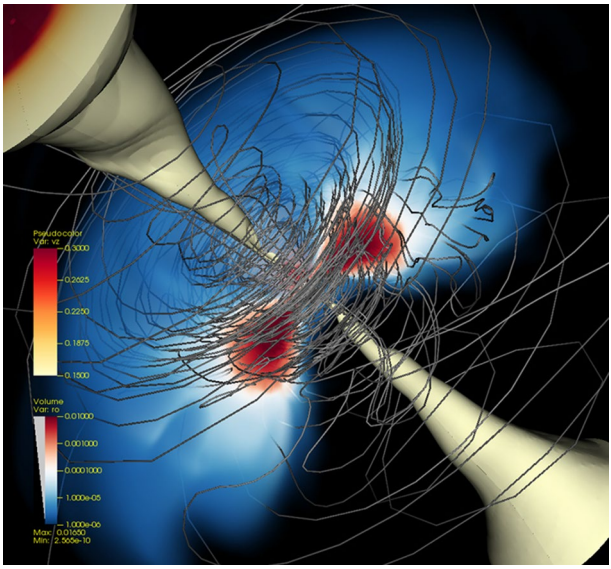

Fig. 11 Simulation of the global structure of radiation-dominated accretion disks near a black hole showing the density (bluewhitered volume rendering), the outflow velocity (whitered rendering), and the magnetic field lines (gray lines). Taken from Takahashi et al. (2016)

several times the neutron star radius. The plasma falls to the two magnetic poles of the neutron star along the dipole magnetic field, forming accretion columns. The simulation results support the hypothesis that the observed ultraluminous X-ray pulsars are powered by the supercritical accretion onto the magnetized neutron stars.

Astrophysical dynamos in rotating disks Magnetic field is ubiquitous in astrophysical systems, from the Sun (as mentioned above) to galaxies (Han 2017). Differential rotation plays an important role in the global dynamo process, at least in the case of the Sun. The differential rotation exists in the solar convection zone as well as the accretion disks, or galactic disks. In the case of these disks which rotate around the z-axis, the dynamo mechanism works in such a closed loop of processes: (1) owing to the magnetorotational instability, any weak vertical magnetic field (B_z) will generate the radial magnetic field (B_r); (2) owing to the differential rotation, the radial component of the magnetic field will generate the azimuthal component (B_ϕ) (note that the generated B_ϕ has a feedback to B_r subject to the magnetorotational instability); (3) once the azimuthal magnetic field is amplified to a certain level, the magnetic field lines rise up from the disk to form magnetic loops due to the Parker instability, so as to enhance B_z.

Machida et al. (2013) carried out global 3D MHD simulations of the dynamo activities in galactic disks, as shown in Fig. 12a. They revealed that in steps (1) and (2), the mean strength of the magnetic field can be amplified until the magnetic pressure becomes ∼10% of the gas pressure. At local areas with a plasma β less than 5 near the disk surface, magnetic flux escapes from the disk by the Parker instability

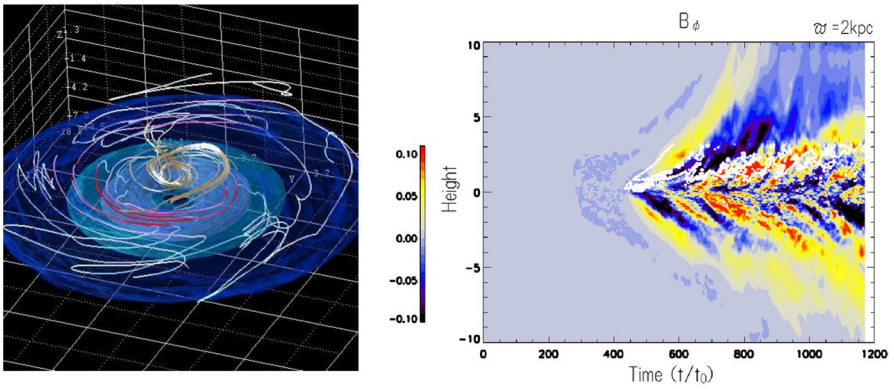

Fig. 12 Panel a: density distribution (isosurface) and magnetic field lines (solid lines) of the simulated galactic disk. Panel b: time evolution of the azimuthal component of the magnetic field averaged in the azimuthal direction. Adapted from Machida et al. (2013)

within a rotation period. The direction of the azimuthal magnetic field B_ϕ reverses quasi-periodically on a timescale of ten rotation periods, as seen in Fig. 12b.

Winds from black hole accretion disks Accretion is an extremely efficient energy conversion mechanism, with an efficiency even higher than nuclear fusion. Hence it is applied to explain many eruptive objects, such as quasars, AGNs or black hole X-ray binaries. Several accretion models have been proposed (Yuan and Narayan 2014), including the standard thin disk and hot accretion flow models. Whereas relativistic jets have been directly observed and winds were also detected in thin accretion disks, one interesting question is whether winds exist outside the hot accretion disks.

Interestingly, hydrodynamic simulations performed by several groups indicated that the accretion rate in the hot accretion disk becomes smaller as the accretion flows move closer to the central black hole. Where has the accretion mass gone? To solve this problem, two interpretations have been proposed: Most people believed that the decreasing accretion rate is because some of the accreting plasmas are pushed away from the disk to form winds (or called outflows). Some authors claimed that the accreting flow is convectively unstable, and the convective flow contributes partly to the decreasing accretion rate. To clarify it, Yuan et al. (2012, 2015) performed hydrodynamic and MHD simulations, in which they traced the trajectories of 100 test particles and found that most of the accretion flow escapes in the form of winds, rather than convection flows as illustrated by the particle trajectories in Fig. 13. Detailed analysis indicates that the driving forces of the winds are the combination of the centrifugal force and the gradient of the gas and magnetic pressure. The existence of the winds from Sgr A* was later confirmed with Chandra observations (Wang et al. 2013).

Further simulations suggest that strong winds exist mainly within the Bondi radius of the hot accretion flow (Bu et al. 2016a, b).

Star and circumstellar disk formation It is generally believed that a molecular cloud core would naturally collapse to a star subject to the Jeans instability. Owing

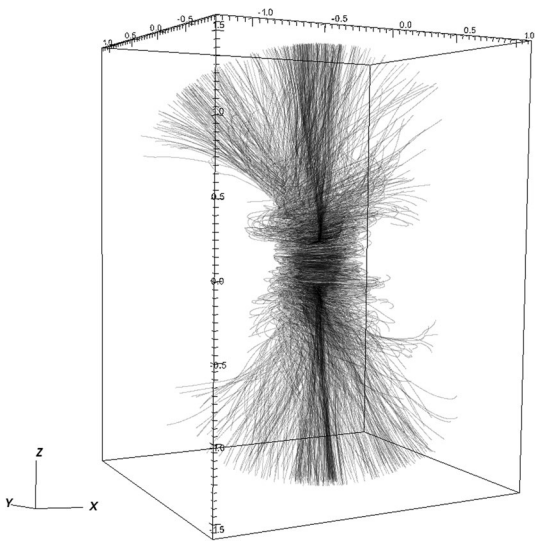

Fig. 13 Trajectories of 100 test particles from the simulated accretion disk, showing that most of the particles escape from the disk in the form of winds. Taken from Yuan et al. (2015)

to the inherent angular momentum, a circumstellar disk is expected to form as a by-product. On the one hand, the disk is the reservoir for the planets orbiting the central star; on the other hand, a disk plays crucial roles in the star formation and evolution. A self-consistent model should explain the formation of the star and the circumstellar disk simultaneously. However, the modeling has been confronted with three difficulties: (1) the initial angular momentum of the molecular cloud is far too larger than that of the formed star; (2) the magnetic flux of the molecular cloud is far too larger than that of the star; (3) magnetic field can transport angular momentum so as to relieve the first difficulty, but the problem is that the transport efficiency is so high that a circumstellar disk cannot survive, which is called the magnetic braking crisis.

Tomida et al. (2015) performed 3D radiation MHD simulations of protostellar collapse with non-ideal effects included, such as Ohmic dissipation and ambipolar diffusion. They found that Ohmic dissipation works in the high density region within the first core and suppresses angular momentum transport, leading to the formation of a disk after the second collapse. With both Ohmic dissipation and ambipolar diffusion, magnetic flux is lost significantly while keeping a circumstellar disk, as illustrated in Fig. 14. It means that the non-ideal effects can solve the magnetic braking crisis.

In the above-mentioned work, the resulting disk is still too small in size, i.e., only 5 AU at the end of the first core phase. Tomida et al. (2017) extended the simulation to a much longer time. It is seen that as accretion continues, and the radius of the circumstellar disk grows to ~200 AU. During the growth, a pair of grand-design spiral arms is formed repeatedly due to the gravitational instability, with a period of a few orbits. The arms can transport angular momentum by gravitational torque. They argued that young circumstellar disks should be massive, e.g., 30–40% of the stellar mass.

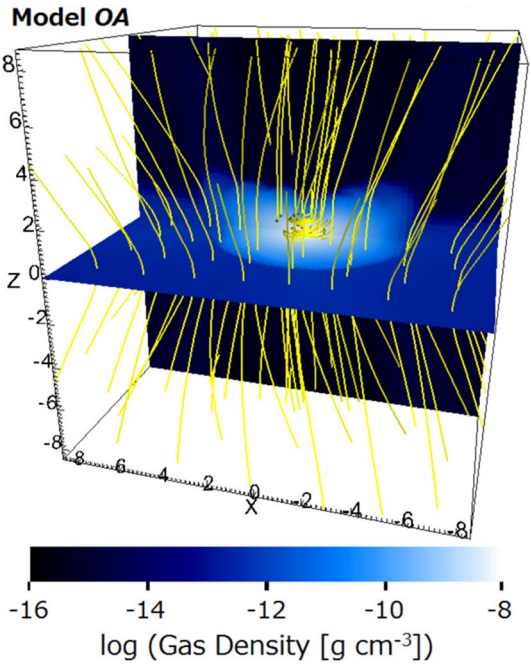

Fig. 14 Magnetic field (yellow lines) and density (color) distributions in the simulation where both Ohmic heating and ambipolar diffusion are considered. Taken from Tomida et al. (2015)

Shocks Shock waves exist in various astrophysical processes, such as solar eruptions and supernovae. Not only can they efficiently accelerate particles to relativistic energies and heat the plasma into γ-ray emitting temperatures, but also they can compress molecular clouds so as to trigger star formation. Six talks about shock waves were presented in this meeting.

Low Mach-number shocks appear typically in the solar–terrestrial system and the late-phase supernova remnants. They might even exist in sub-structures of young supernova remnants due to the modulation of the cosmic rays accelerated by the shock itself. The reason for the latter case is that the accelerated cosmic rays excite waves in the downstream and upstream of the shock. The waves in the upstream are dissipated, resulting in the local plasma heating, and hence the local Mach number may decrease down to ∼10. Umeda et al. (2012, 2014) performed 2D PIC simulations, where they found that when the ion-to-electron mass ratio is large, the modified two-stream instability dominates in generating whistler-mode waves. The waves propagating downstream are more enhanced at the foot of the shock ripples. These waves modify the dynamics of the collisionless shock, as illustrated in Fig. 15. Recently, they set up a laboratory experiment to investigate the low Mach-number shock physics (Shoji et al. 2016). The advantages of the setup are: (1) plasma density and temperature across the shock can be simultaneously measured via coherent Thomson scattering; (2) it is easy to excite supercritical shocks with an Alfvén Mach number greater than 3.

Supernova remnants are formed by the interaction between the strong shock wave caused by supernova and the interstellar medium. Some observations in X-rays and

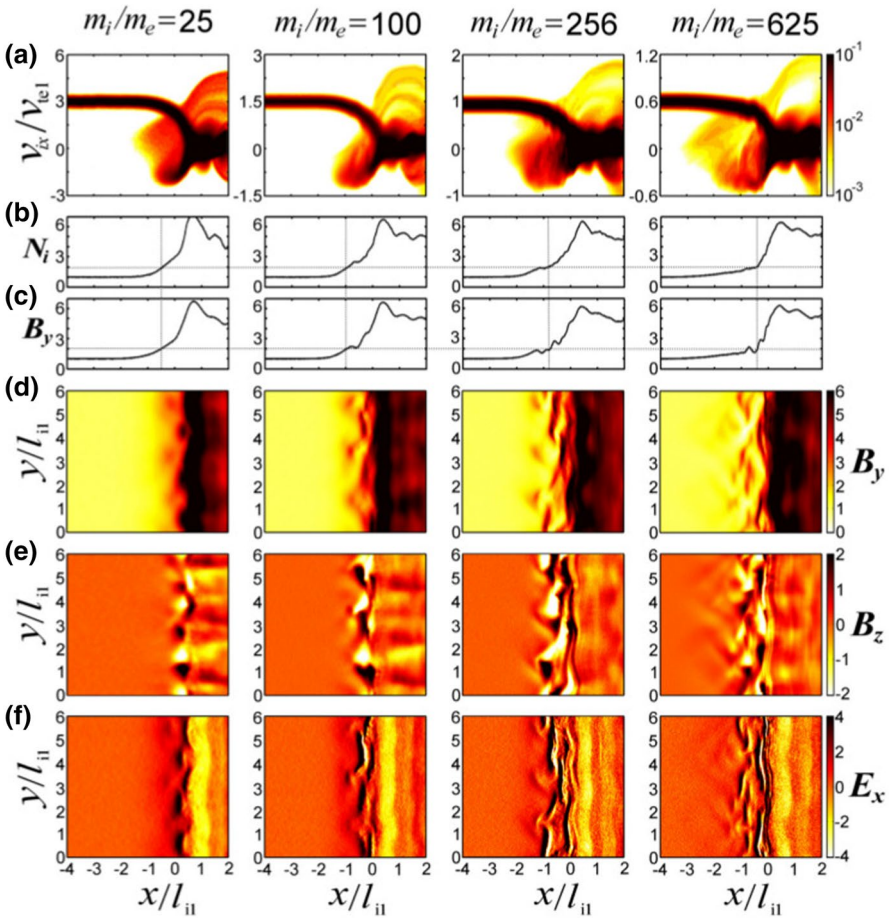

Fig. 15 Structure of the perpendicular shock transition region in a 2D particle-in-cell simulation, showing that whistler-mode waves modify the dynamics of the shock. Taken from Umeda et al. (2014)

γ-rays are puzzling and cannot be explained by the shock interaction with idealized uniform interstellar medium. With 3D radiation MHD simulations, Inoue and Inutsuka (2012) proposed that the flow of the interstellar medium would generate shock waves, behind which the He I medium piles up. Owing to the thermal instability where C II and CO spectral lines dominate the radiative cooling, dense clouds are formed, as demonstrated in Fig. 16.

They argued that the interaction between the supernova shock and the small-scale clumps is crucial. Although the shock decelerates in clouds, it can keep a high speed in the interclouds where it can then accelerate particles. At the same time, the shock–clump interaction leads to the magnetic field amplification due to a process similar to the Ritchmyer–Meshkov instability, resulting in enhanced synchrotron X-ray emission (Sano et al. 2013). The turbulent magnetic field can

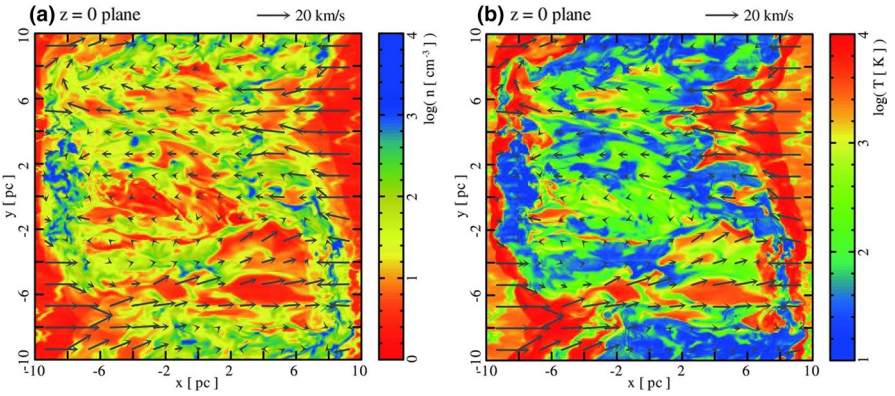

Fig. 16 Distributions of the plasma temperature (color) and the velocity after a shock sweeps the clumpy interstellar medium. Taken from Inoue and Inutsuka (2012)

also prevent the penetration of low-energy cosmic rays into the interstellar clouds, which can then explain the observed hardening of the γ-ray spectrum.

A clumpy interstellar medium is also crucial to maintain the magnetic field amplification behind shock waves. It is known that the Weibel instability in the shock downstream can lead to magnetic field amplification. However, in the case of a uniform upstream interstellar medium, the amplified magnetic field in the downstream decays rapidly. Tomita and Ohira (2016) performed 2D PIC simulations of the interaction between a shock and an inhomogeneous medium. Their results indicate that the amplified magnetic field in the downstream can survive for a longer time. At the same time, because the thermal particles escape anisotropically in the turbulent magnetic field, the plasma temperature in the downstream becomes strongly anisotropic, which can explain the afterglow emission of GRBs.

Observations indicate that both protons and electrons are accelerated to TeV energies in supernova shocks. However, according to the diffusive shock acceleration theory, shocks can efficiently accelerate ions but not electrons, since slow electrons are strongly magnetized and are not scattered by MHD waves. One possible solution is that the electrons are pre-accelerated. In this sense, the shock surfing acceleration becomes important for electrons in the high Mach-number shock case. Two processes might contribute to the electron pre-acceleration: (1) electrostatic waves generated by the Buneman instability at the leading edge of the strong shock; (2) strong turbulence generated by the ion-Weibel instability in the shock transition region. Matsumoto et al. (2017) performed the first 3D PIC simulation of high Mach-number shocks. They found both electrostatic Buneman waves and ion-Weibel magnetic turbulence exist, as shown in Fig. 17, and electrons gain energy mainly from the ion-Weilbel turbulence.

For an electron–positron plasma such as in GRBs, the Weibel turbulence in the shock upstream can excite electromagnetic wave emission via the synchrotron maser instability. Although the electromagnetic emission in 2D PIC simulations is weaker

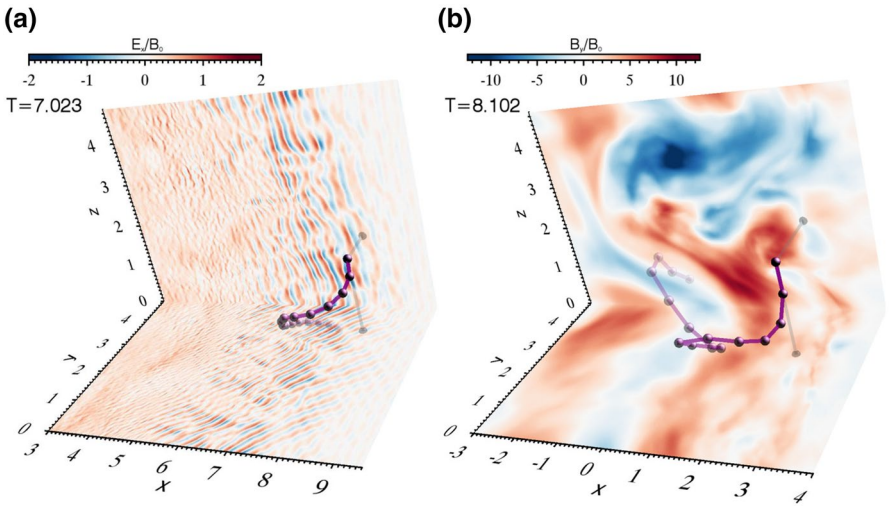

Fig. 17 Trajectory of an electron showing how it is pre-accelerated by the electrostatic waves and magnetic turbulence via the shock surfing mechanism. Taken from Matsumoto et al. (2017)

than in the 1D case, it persists, and is strong enough to disturb the upstream medium (Iwamoto et al. 2017).

Once electrons are accelerated at high Mach-number shocks, they emit synchrotron radiation in radio wavelengths. The spectrum of the fluctuations in the radio images should be strongly coupled with the spectrum of the turbulent magnetic field behind the shock. Using high-resolution radio images of Tycho's supernova remnants, Shimoda (2018) tried to make the inversion of the spectrum of the turbulent magnetic field. They found that only near the outer shell of the remnant the spectrum of the turbulent magnetic field is Kolmogorov-like.

Instrumentation Coronal magnetic field is the key to understanding the mechanisms of solar eruptions, including solar flares (Shibata and Magara 2011) and CMEs (Chen 2011; Webb and Howard 2012). Unfortunately, so far only the photospheric magnetic field at the solar surface can be readily and routinely observed. The coronal magnetic field has to be extrapolated from the solar photosphere with a force-free field model. However, the photosphere is a high plasma-β layer, where the force-free condition is not satisfied. There have been efforts in the past decades to measure the solar magnetic field at higher layers, e.g., the chromosphere and the transition region. Kano et al. (2017) introduced the Chromospheric Lyα Spectro-Polarimeter (CLASP), a sounding rocket mission. Several solar ultraviolet lines were chosen. They detected the scattering polarization in the Lyα at 1216 Å for the first time. It is seen that (1) a few percent of polarization was observed in the Lyα wing, which is ~10 times larger than in the core; (2) a clear center-to-limb variation is discernable in the wing of Stokes Q / I polarization (see Fig. 18), but not in the core.

Recently, the first solar space mission in China, Advanced Space-based Solar Observatory (ASO-S, Gan et al. 2015), was approved by the funding agency. Li from Purple Mountain Observatory introduced the scientific objectives and the optical

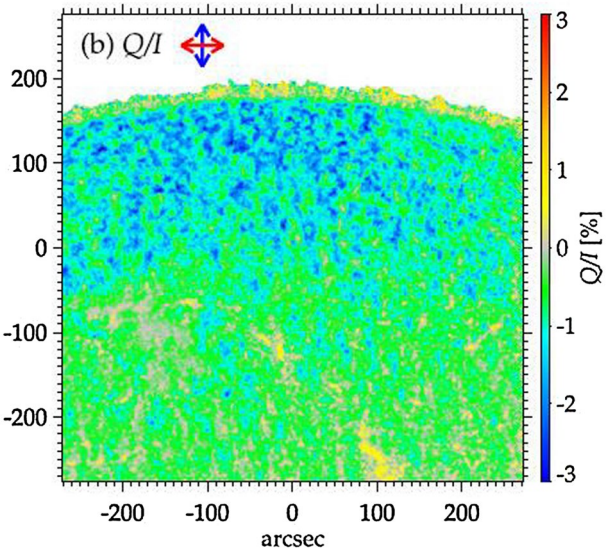

Fig. 18 The Stokes Q / I map of the Sun observed by the CLASP slit-jaw camera. Taken from Kano et al. (2017)

design of the Lyα Solar Telescope (LST, Li 2016), which is one of the three aboard payloads. LST consists of a solar disk imager (SDI) in Lyα with a field of view of $1.2R_{\odot}$, a solar coronal imager (SCI) in Lyα with a field of view of $1.1–2.5R_{\odot}$, and a full-disk white-light solar telescope (WST), with the same field of view as SDI.

The discovery of gravitational waves opened up an irreplaceable new window to look into some astrophysical dynamics in the deep space (Abbott et al. 2016). However, there is still a long way to go for gravitational-wave astronomy to mature, since the capability of the existing facilities, e.g., the Laser Interferometer Gravitation Wave Observatory (LIGO), is still limited. We need to build a global array on the ground and in space as well. Recently, the Indian government flagged off the LIGO-India project. In his plenary talk, T. Souradeep reviewed the momentous discovery of gravitational waves, the prospect of gravitational-wave astronomy, and the status of LIGO-India.

Laboratory plasma experiments Hui Li from Los Alamos National Laboratory gave a plenary talk on laboratory plasma experiments, which tried to reproduce astrophysical structures and eruptions. For example, they compared the jets in spheromaks and astrophysical jets, by which they proposed that the cosmic rays might be accelerated by the drift cyclotron loss cone kinetic instability (Fowler and Li 2016).

Magnetic reconnection is a process widely investigated in laboratory plasma experiments. Besides reviewing recent progress on this topic, Zhong et al. (2016) also displayed their new results obtained with the Chinese Shenguang II laser facility, which can deliver a total energy of 2 kJ in a nanosecond square pulse. Relativistic electrons with energies up to several MeV are detected along the magnetic separatrix. With the inclusion of guide magnetic field in the reconnection site,

more electrons are accelerated. Hardening of the spectrum at energies above 500 keV is seen, which mimics the double power-law energy spectrum observed in solar flares. As shown in Fig. 19, the high energy particles are ejected nearly symmetrically along the current sheet direction in the case without a guide field; they become asymmetric when there is a guide magnetic field.

Lee (2018) introduced their experiments of magnetic reconnection using a Peta–Watt laser facility in Korea. They found that argon ions are ionized to a charge state up to 4+, and the ions are accelerated only in the direction transverse to the laser beam, which is puzzling.

Numerical code A new MHD numerical code, called CANS+, was recently developed by Matsumoto et al. (2016). The code implements the HLLD approximate Riemann solver and the fifth-order interpolation scheme, which significantly improved the numerical accuracy and stability. Numerical experiments indicate that the performance of the new scheme is better than a standard second-order TVD scheme because the same accuracy can be attained with a smaller number of grid points. The new code allows to explore long-term evolution. Considering that a dense gas cloud about three times the mass of Earth was observed to fall into the accretion region of Sgr A* 6 years ago, these authors used this code to simulate the interaction between the gas cloud and the black hole accretion system. Based on the simulation results, they predict that there will be much enhanced radio emission from Sgr A* in 5–10 years (Kawashima et al., 2017).

Challenging the orthodox Almost more than 30 years ago, there was a two-step paradigm for solar flares and CMEs: (1) subject to ideal MHD instabilities, the nonpotential magnetic field is pulled up by its own Lorentz force to form open magnetic field in the interplanetary space, forming an elongated current sheet above the magnetic neutral line; (2) the ensuing magnetic reconnection of the current sheet leads to a solar flare near the solar surface and a CME erupting away from the Sun. However, Aly (1991) and Sturrock (1991) argued that the process in step (1) is forbidden since the magnetic energy of the open field is larger than any force-free field with the field lines being tied to the solar surface, if all the magnetic field lines are simply connected, i.e., they are neither knotted nor detached from the solar surface. In his talk, Choe (2018) argues that the proof of Aly–Sturrock theorem is based on a few explicit and implicit assumptions, which can be readily discarded. He further constructed a sequence of force-free

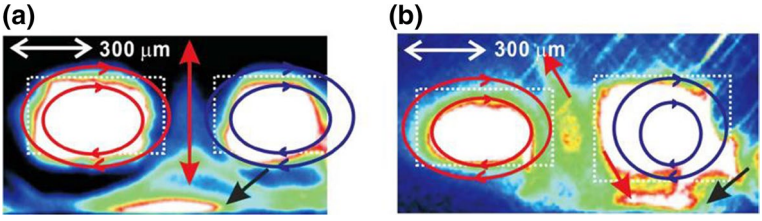

Fig. 19 Energetic electrons accelerated in the magnetic reconnection without a guide magnetic field (left panel) and with a guide field (right panel). Taken from Zhong et al. (2016)

magnetic field by moving the footpoints of the magnetic loops, where the magnetic energy surpasses the energy of the corresponding open field.

Melrose (2018) also argues that one key ingredient that is missing in most flare models is the electromotive force, which is a global parameter. With the inclusion of the electromotive force, many puzzles in flare physics can be solved, such as the number problem of the nonthermal electrons.

3 Summary

The First Asia-Pacific Conference on Plasma Physics was held successfully in Chengdu, China, during September 18–23, 2017. The Solar/Astron Session contributed significantly to the success of the conference with fruitful discussions inside the session itself and in the plenary part. Based on this review, we can see that, whereas even the Solar/Astron session covered a diversity of topics from the Sun to the galaxies and accretion disks, there are common fundamental problems among them, such as magnetic reconnection, particle acceleration, waves and instabilities, and dynamos. For example, we have seen that the dynamo mechanism in galactic disks (Machida et al. 2013) is so much similar to the Babcock–Leighton model for the solar dynamo. As a second example, cool material embedded in hot plasma due to thermal instability is a common process inside the solar corona (with a length scale of $R_\odot \sim 6.9 \times 10^5$ km, Chen et al. 2014b) and the corona of galaxy clusters (with a length scale of 10 kpc$\sim 3 \times 10^{17}$ km, Prasad et al. 2015). The investigation on their formation and maintenance would be beneficial to both communities, and the extension from solar flares to stellar superflares has set up an excellent paradigm in this sense (Shibata et al. 2013). Moreover, many of these problems can be studied in laboratory plasma experiments. Putting all these communities together is the main initiative of this conference.

Acknowledgements The authors are grateful to Prof. M. Kikuchi for the invitation to write this summary paper, and to the referees for their detailed suggestions. PFC was supported by the Chinese foundations (NSFC 11533005 and BRA2017359).

References

B.P. Abbott, R. Abbott, T.D. Abbott, M.R. Abernathy, F. Acernese, K. Ackley, C. Adams, T. Adams, P. Addesso, R.X. Adhikari et al., Observation of gravitational waves from a binary black hole merger. Phys. Rev. Lett. **116**(6), 061102 (2016). https://doi.org/10.1103/PhysRevLett.116.061102,1602.03837

J.J. Aly, How much energy can be stored in a three-dimensional force-free magnetic field? ApJL **375**, L61–L64 (1991). https://doi.org/10.1086/186088

T.E. Berger, R.A. Shine, G.L. Slater et al., Hinode SOT observations of solar quiescent prominence dynamics. ApJL **676**, L89 (2008). https://doi.org/10.1086/587171

Y. Bi, Y. Jiang, J. Yang, J. Hong, H. Li, B. Yang, Z. Xu, Observation of a reversal of rotation in a sunspot during a solar flare. Nat. Commun. **7**, 13798 (2016). https://doi.org/10.1038/ncomms13798

Y. Bi, J. Yang, Y. Jiang, J. Hong, Z. Xu, Z. Qu, K. Ji, The photospheric vortex flows during a solar flare. ApJL **849**, L35 (2017). https://doi.org/10.3847/2041-8213/aa960e

D.F. Bu, F. Yuan, Z.M. Gan, X.H. Yang, Hydrodynamical numerical simulation of wind production from black hole hot accretion flows at very large radii. ApJ **818**, 83 (2016a). https://doi.org/10.3847/0004-637X/818/1/83. 1510.03124

D.F. Bu, F. Yuan, Z.M. Gan, X.H. Yang, Magnetohydrodynamic numerical simulation of wind production from hot accretion flows around black holes at very large radii. ApJ **823**, 90 (2016b). https://doi.org/10.3847/0004-637X/823/2/90. 1603.09442

L. Chen, D.J. Wu, G.Q. Zhao, J.F. Tang, J. Huang, Excitation of Kinetic Alfvén waves by fast electron beams. ApJ **793**, 13 (2014a). https://doi.org/10.1088/0004-637X/793/1/13

P.F. Chen, Coronal mass ejections: models and their observational basis. Living Rev. Sol. Phys. **8**, 1 (2011). https://doi.org/10.12942/lrsp-2011-1

P.F. Chen, K. Shibata, An emerging flux trigger mechanism for coronal mass ejections. ApJ **545**, 524–531 (2000). https://doi.org/10.1086/317803

P.F. Chen, L.K. Harra, C. Fang, Imaging and spectroscopic observations of a filament channel and the implications for the nature of counter-streamings. ApJ **784**, 50 (2014b). https://doi.org/10.1088/0004-637X/784/1/50.1401.4514

G.S. Choe, Revisiting the Aly-Sturrock constraint. ApJ (2018). In preparation

A.R. Choudhuri, Starspots, stellar cycles and stellar flares: lessons from solar dynamo models. Sci. China Phys., Mech. Astron. **60**(1), 19601 (2017). https://doi.org/10.1007/s11433-016-0413-7.1612.02544

Y. Fan, F. Fang, A simulation of convective dynamo in the solar convective envelope: maintenance of the solar-like differential rotation and emerging flux. ApJ **789**, 35 (2014). https://doi.org/10.1088/0004-637X/789/1/35.1405.3926

J. Feynman, S.F. Martin, The initiation of coronal mass ejections by newly emerging magnetic flux. JGR **100**, 3355–3367 (1995). https://doi.org/10.1029/94JA02591

T.K. Fowler, H. Li, Spheromaks and how plasmas may explain the ultra high energy cosmic ray mystery. J. Plasma Phys. **82**(5), 595820503 (2016). https://doi.org/10.1017/S0022377816000866

W. Gan , Y. Deng, H. Li, et al, ASO-S: advanced space-based solar observatory. in *Proceedings of the SPIE Solar Physics and Space Weather Instrumentation VI*, vol. 9604, p. 96040T. https://doi.org/10.1117/12.2189062

M. Ghizaru, P. Charbonneau, P.K. Smolarkiewicz, Magnetic cycles in global large-eddy simulations of solar convection. ApJL **715**, L133–L137 (2010). https://doi.org/10.1088/2041-8205/715/2/L133

Y. Guo, B. Schmieder, P. Démoulin, T. Wiegelmann, G. Aulanier, T. Török, V. Bommier, Coexisting flux rope and dipped arcade sections along one solar filament. ApJ **714**, 343–354 (2010). https://doi.org/10.1088/0004-637X/714/1/343

J.L. Han, Observing interstellar and intergalactic magnetic fields. ARAA **55**, 111–157 (2017). https://doi.org/10.1146/annurev-astro-091916-055221

A. Hillier, The magnetic Rayleigh–Taylor instability in solar prominences. Rev. Mod. Plasma Phys. **2**, 1 (2018). https://doi.org/10.1007/s41614-017-0013-2

A. Hillier, T. Berger, H. Isobe, K. Shibata, Numerical simulations of the Magnetic Rayleigh–Taylor instability in the Kippenhahn–Schlüter prominence model. I. Formation of upflows. ApJ **746**, 120 (2012a). https://doi.org/10.1088/0004-637X/746/2/120

A. Hillier, R. Hillier, D. Tripathi, Determination of prominence plasma β from the dynamics of rising plumes. ApJ **761**, 106 (2012b). https://doi.org/10.1088/0004-637X/761/2/106.1211.0742

H. Hotta, M. Rempel, T. Yokoyama, Large-scale magnetic fields at high Reynolds numbers in magnetohydrodynamic simulations. Science **351**, 1427–1430 (2016). https://doi.org/10.1126/science.aad1893

H. Iijima, T. Yokoyama, Effect of coronal temperature on the scale of solar chromospheric jets. ApJL **812**, L30 (2015). https://doi.org/10.1088/2041-8205/812/2/L30.1509.06677

H. Iijima, T. Yokoyama, A three-dimensional magnetohydrodynamic simulation of the formation of solar chromospheric jets with twisted magnetic field lines. ApJ **848**, 38 (2017). https://doi.org/10.3847/1538-4357/aa8ad1.1709.01522

T. Inoue, Inutsuka Si, Formation of turbulent and magnetized molecular clouds via accretion flows of H I clouds. ApJ **759**, 35 (2012). https://doi.org/10.1088/0004-637X/759/1/35.1205.6217

N. Ishiguro, K. Kusano, Double arc instability in the solar corona. ApJ **843**, 101 (2017). https://doi.org/10.3847/1538-4357/aa799b.1706.06112

M. Iwamoto, T. Amano, M. Hoshino, Y. Matsumoto, Persistence of precursor waves in two-dimensional relativistic shocks. ApJ **840**, 52 (2017). https://doi.org/10.3847/1538-4357/aa6d6f.1704.04411

R. Kano, J. Trujillo Bueno, A. Winebarger et al., Discovery of scattering polarization in the hydrogen Lyα line of the solar disk radiation. ApJL **839**, L10 (2017). https://doi.org/10.3847/2041-8213/aa697f.1704.03228

T. Kawashima, Y. Matsumoto, R. Matsumoto, A possible time-delayed brightening of the Sgr A* accretion flow after the pericenter passage of the G2 cloud. PASJ **69**, 43 (2017). https://doi.org/10.1093/pasj/psx015.1702.07903

J.A. Klimchuk, Key aspects of coronal heating. Philos. Trans. R. Soc. Lond. Ser. A **373**, 20140256 (2015). https://doi.org/10.1098/rsta.2014.0256,1410.5660

K. Kusano, Y. Bamba, T.T. Yamamoto, Y. Iida, S. Toriumi, A. Asai, Magnetic field structures triggering solar flares and coronal mass ejections. ApJ **760**, 31 (2012). https://doi.org/10.1088/0004-637X/760/1/31.1210.0598

B.R. Lee, Magnetic reconnection. Plasma Science and Technology (2018). In preparation

H. Li, The Lyman-α solar telescope (LST) for the ASO-S mission. in *IAU Symposium Solar and Stellar Flares and their Effects on Planets*, vol. 320, ed. by A.G. Kosovichev, S.L. Hawley, P. Heinzel, pp. 436–438 (2016), https://doi.org/10.1017/S1743921316000533

J. Li, W. Zhong, Summary of magnetic fusion plasma physics in 1st AAPPS-DPP meeting. Rev. Mod. Plasma Phys. **2**, 3 (2018). https://doi.org/10.1007/s41614-018-0015-8

R.P. Lin, WIND observations of suprathermal electrons in the interplanetary medium. SSR **86**, 61–78 (1998). https://doi.org/10.1023/A:1005048428480

M. Machida, K.E. Nakamura, T. Kudoh, T. Akahori, Y. Sofue, R. Matsumoto, Dynamo activities driven by magnetorotational instability and the parker instability in galactic gaseous disks. ApJ **764**, 81 (2013). https://doi.org/10.1088/0004-637X/764/1/81.1301.1414

H. Maehara, T. Shibayama, S. Notsu et al., Superflares on solar-type stars. Nature **485**, 478–481 (2012). https://doi.org/10.1038/nature11063

S.F. Martin, Conditions for the formation and maintenance of filaments (Invited Review). Sol. Phys. **182**, 107–137 (1998). https://doi.org/10.1023/A:1005026814076

S.F. Martin, R. Bilimoria, P.W. Tracadas, Magnetic field configurations basic to filament channels and filaments. in: *NATO Advanced Science Institutes (ASI) Series C, NATO Advanced Science Institutes (ASI) Series C*, vol 433, ed. by R.J. Rutten, C.J. Schrijver (1994), p. 303

Y. Masada, T. Sano, Spontaneous formation of surface magnetic structure from large-scale dynamo in strongly stratified convection. ApJL **822**, L22 (2016). https://doi.org/10.3847/2041-8205/822/2/L22.1604.05374

Y. Masada, T. Sano, The compression effect. ApJ (2018). In preparation

Y. Matsumoto, Y. Asahina, Y. Kudoh, T. Kawashima, J. Matsumoto, H.R. Takahashi, T. Minoshima, S. Zenitani, T. Miyoshi, R. Matsumoto, Magnetohydrodynamic Simulation Code CANS+: Assessments and Applications. ArXiv e-prints **1611**, 01775 (2016)

Y. Matsumoto, T. Amano, T.N. Kato, M. Hoshino, Electron surfing and drift accelerations in a Weibel-dominated high-mach-number shock. Phys. Rev. Lett. **119**(10), 105101 (2017). https://doi.org/10.1103/PhysRevLett.119.105101

D.B. Melrose, Rethinking the solar flare paradigm. Plasma Sci. Tech. **20**, 074003 (2018). (1803.10389)

J. Muhamad, K. Kusano, S. Inoue, D. Shiota, Magnetohydrodynamic simulations for studying solar flare trigger mechanism. ApJ **842**, 86 (2017). https://doi.org/10.3847/1538-4357/aa750e.1706.07153

T.J. Okamoto, P. Antolin, B. De Pontieu, H. Uitenbroek, T. Van Doorsselaere, T. Yokoyama, Resonant absorption of transverse oscillations and associated heating in a solar prominence. I. Observational aspects. ApJ **809**, 71 (2015). https://doi.org/10.1088/0004-637X/809/1/71.1506.08965

Y. Ouyang, Y.H. Zhou, P.F. Chen, C. Fang, Chirality and magnetic configurations of solar filaments. ApJ **835**, 94 (2017). https://doi.org/10.3847/1538-4357/835/1/94.1612.01054

A. Pouquet, U. Frisch, J. Leorat, Strong MHD helical turbulence and the nonlinear dynamo effect. J. Fluid Mech. **77**, 321–354 (1976). https://doi.org/10.1017/S0022112076002140

D. Prasad, P. Sharma, A. Babul, Cool core cycles: cold gas and AGN jet feedback in cluster cores. ApJ **811**, 108 (2015). https://doi.org/10.1088/0004-637X/811/2/108.1504.02215

D. Prasad, P. Sharma, A. Babul, AGN jet-driven stochastic cold accretion in cluster cores. MNRAS **471**, 1531–1542 (2017). https://doi.org/10.1093/mnras/stx1698.1611.02710

M. Ryutova, T. Berger, Z. Frank, T. Tarbell, A. Title, Observation of plasma instabilities in quiescent prominences. Sol. Phys. **267**, 75–94 (2010). https://doi.org/10.1007/s11207-010-9638-9

H. Sano, T. Tanaka, K. Torii, T. Fukuda, S. Yoshiike, J. Sato, H. Horachi, T. Kuwahara, T. Hayakawa, H. Matsumoto, T. Inoue, R. Yamazaki, S. Inutsuka, A. Kawamura, K. Tachihara, H. Yamamoto, T. Okuda, N. Mizuno, T. Onishi, A. Mizuno, Y. Fukui, Non-thermal X-Rays and interstellar gas toward

the γ-Ray supernova remnant RX J1713.7-3946: evidence for X-ray enhancement around CO and H I clumps. ApJ **778**, 59 (2013). https://doi.org/10.1088/0004-637X/778/1/59,1304.7722
N. Seehafer, Electric current helicity in the solar atmosphere. Sol. Phys. **125**, 219–232 (1990). https://doi.org/10.1007/BF00158402
J. Seough, Y. Nariyuki, P.H. Yoon, S. Saito, Strahl formation in the solar wind electrons via whistler instability. ApJL **811**, L7 (2015). https://doi.org/10.1088/2041-8205/811/1/L7
Y. Shen, Y. Liu, Y.D. Liu, P.F. Chen, J. Su, Z. Xu, Z. Liu, Fine magnetic structure and origin of counter-streaming mass flows in a quiescent solar prominence. ApJL **814**, L17 (2015). https://doi.org/10.1088/2041-8205/814/1/L17.1511.02489
K. Shibata, T. Magara, Solar flares: magnetohydrodynamic processes. Living Rev. Sol. Phys. **8**, 6 (2011). https://doi.org/10.12942/lrsp-2011-6
K. Shibata, Y. Ishido, L.W. Acton et al., Observations of X-ray jets with the YOHKOH Soft X-ray Telescope. PASJ **44**, L173–L179 (1992)
K. Shibata, T. Nakamura, T. Matsumoto et al., Chromospheric anemone jets as evidence of ubiquitous reconnection. Science **318**, 1591 (2007). https://doi.org/10.1126/science.1146708.0810.3974
K. Shibata, H. Isobe, A. Hillier, A.R. Choudhuri, H. Maehara, T.T. Ishii, T. Shibayama, S. Notsu, Y. Notsu, T. Nagao, S. Honda, D. Nogami, Can superflares occur on our sun? PASJ **65**, 49 (2013). https://doi.org/10.1093/pasj/65.3.49,1212.1361
J. Shimoda, Solar dynamo. ApJ. (2018) In preparation
Y. Shoji, R. Yamazaki, S. Tomita et al., Toward the generation of magnetized collisionless shocks with high-power lasers. Plasma and Fusion Res. **11**(2), 3401031 (2016). https://doi.org/10.1585/pfr.11.3401031
P.A. Sturrock, Maximum energy of semi-infinite magnetic field configurations. ApJ **380**, 655–659 (1991). https://doi.org/10.1086/170620
H.R. Takahashi, K. Ohsuga, General relativistic radiation MHD simulations of supercritical accretion onto a magnetized neutron star: modeling of ultraluminous X-ray pulsars. ApJL **845**, L9 (2017). https://doi.org/10.3847/2041-8213/aa8222.1707.07356
H.R. Takahashi, K. Ohsuga, T. Kawashima, Y. Sekiguchi, Formation of overheated regions and truncated disks around black holes: three-dimensional general relativistic radiation-magnetohydrodynamics simulations. ApJ **826**, 23 (2016). https://doi.org/10.3847/0004-637X/826/1/23.1605.04992
M. Takamoto, A. Lazarian, Compressible relativistic magnetohydrodynamic turbulence in magnetically dominated plasmas and implications for a strong-coupling regime. ApJL **831**, L11 (2016). https://doi.org/10.3847/2041-8205/831/2/L11.1610.01373
M. Takamoto, T. Inoue, A. Lazarian, Turbulent reconnection in relativistic plasmas and effects of compressibility. ApJ **815**, 16 (2015). https://doi.org/10.1088/0004-637X/815/1/16.1509.07703
S. Takeshige, H. Takahashi, K. Shibata, The compression effect. ApJ (2018). In preparation
B. Tan, C. Tan, Microwave quasi-periodic pulsation with millisecond bursts in a solar flare on 2011 august 9. ApJ **749**, 28 (2012). https://doi.org/10.1088/0004-637X/749/1/28,1202.1578
J. Tao, L. Wang, Q. Zong, G. Li, C.S. Salem, R.F. Wimmer-Schweingruber, J. He, C. Tu, S.D. Bale, Quiet-time suprathermal (0.1-1.5 keV) electrons in the solar wind. ApJ **820**, 22 (2016). https://doi.org/10.3847/0004-637X/820/1/22
H. Tian, E.E. DeLuca, S.R. Cranmer et al., Prevalence of small-scale jets from the networks of the solar transition region and chromosphere. Science **346**(27), 1255711 (2014). https://doi.org/10.1126/science.1255711.1410.6143
K. Tomida, S. Okuzumi, M.N. Machida, Radiation magnetohydrodynamic simulations of protostellar collapse: nonideal magnetohydrodynamic effects and early formation of circumstellar disks. ApJ **801**, 117 (2015). https://doi.org/10.1088/0004-637X/801/2/117.1501.04102
K. Tomida, M.N. Machida, T. Hosokawa, Y. Sakurai, C.H. Lin, Grand-design spiral arms in a young forming circumstellar disk. ApJL **835**, L11 (2017). https://doi.org/10.3847/2041-8213/835/1/L11.1611.09361
S. Tomita, Y. Ohira, Weibel instability driven by spatially anisotropic density structures. ApJ **825**, 103 (2016). https://doi.org/10.3847/0004-637X/825/2/103.1606.03213
T. Umeda, Y. Kidani, S. Matsukiyo, R. Yamazaki, Microinstabilities at perpendicular collisionless shocks: a comparison of full particle simulations with different ion to electron mass ratio. Phys. Plasmas **19**(4), 042109 (2012). https://doi.org/10.1063/1.3703319,1204.2539
T. Umeda, Y. Kidani, S. Matsukiyo, R. Yamazaki, Dynamics and microinstabilities at perpendicular collisionless shock: a comparison of large-scale two-dimensional full particle simulations with different

ion to electron mass ratio. Phys. Plasmas **21**(2), 022102 (2014). https://doi.org/10.1063/1.4863836.1401.5903

Y. Voitenko, J. de Keyser, Turbulent spectra and spectral kinks in the transition range from MHD to kinetic Alfvén turbulence. Nonlinear Process. Geophys. **18**, 587–597 (2011). https://doi.org/10.5194/npg-18-587-2011.1105.1941

L. Wang, L. Yang, J. He et al., Solar wind 20–200 keV superhalo electrons at quiet times. ApJL **803**, L2 (2015). https://doi.org/10.1088/2041-8205/803/1/L2

Q.D. Wang, M.A. Nowak, S.B. Markoff et al., Dissecting X-ray-emitting gas around the center of our galaxy. Science **341**, 981–983 (2013). https://doi.org/10.1126/science.1240755,1307.5845

D.F. Webb, T.A. Howard, Coronal mass ejections: observations. Living Rev. Sol. Phys. **9**, 3 (2012). https://doi.org/10.12942/lrsp-2012-3

O.C. Wilson, Chromospheric variations in main-sequence stars. ApJ **226**, 379–396 (1978). https://doi.org/10.1086/156618

D.J. Wu, L. Chen, Excitation of Kinetic Alfvén waves by density striation in magneto-plasmas. ApJ **771**, 3 (2013). https://doi.org/10.1088/0004-637X/771/1/3

L. Xiang, D.J. Wu, L. Chen, Excitation of Ion cyclotron waves by ion and electron beams in compensated-current system. ApJ **857**, 108 (2018). https://doi.org/10.3847/1538-4357/aab662

H. Xie, M.S. Madjarska, B. Li, Z. Huang, L. Xia, T. Wiegelmann, H. Fu, C. Mou, The plasma parameters and geometry of cool and warm active region loops. ApJ **842**, 38 (2017). https://doi.org/10.3847/1538-4357/aa7415.1705.02564

F. Yuan, R. Narayan, Hot accretion flows around black holes. ARAA **52**, 529–588 (2014). https://doi.org/10.1146/annurev-astro-082812-141003.1401.0586

F. Yuan, M. Wu, D. Bu, Numerical simulation of hot accretion flows. I. A large radial dynamical range and the density profile of Accretion Flow. ApJ **761**, 129 (2012). https://doi.org/10.1088/0004-637X/761/2/129,1206.4157

F. Yuan, Z. Gan, R. Narayan, A. Sadowski, D. Bu, X.N. Bai, Numerical simulation of hot accretion flows. III. Revisiting wind properties using the trajectory approach. ApJ **804**, 101 (2015). https://doi.org/10.1088/0004-637X/804/2/101,1501.01197

M. Zhang, Y. Fan, Solar dynamo. ApJ (2018). In preparation

J.S. Zhao, Y. Voitenko, D.J. Wu, J. De Keyser, Nonlinear Generation of kinetic-scale waves by magneto-hydrodynamic Alfvén waves and nonlocal spectral transport in the solar wind. ApJ **785**, 139 (2014). https://doi.org/10.1088/0004-637X/785/2/139

J.Y. Zhong, J. Lin, Y.T. Li et al., Relativistic electrons produced by reconnecting electric fields in a laser-driven bench-top solar flare. ApJS **225**, 30 (2016). https://doi.org/10.3847/0067-0049/225/2/30

J.Z. Zhu, Chirality, extended magnetohydrodynamics statistics and topological constraints for solar wind turbulence. MNRAS **470**, L87–L91 (2017). https://doi.org/10.1093/mnrasl/slx075

P. Zou, C. Fang, P.F. Chen, K. Yang, W. Cao, Magnetic separatrix as the source region of the plasma supply for an active-region filament. ApJ **836**, 122 (2017). https://doi.org/10.3847/1538-4357/836/1/1221701.01526